Acta Crystallographica Section B
Structural Science
ISSN 0108-7681

Anisotropic crystal structure distortion of the monoclinic polymorph of acetaminophen at high hydrostatic pressures

E. V. Boldyreva,[a,b]* T. P. Shakhtshneider,[a] M. A. Vasilchenko,[a,b] H. Ahsbahs[c] and H. Uchtmann[c]

[a]Institute of Solid State Chemistry and Mechanochemistry SD RAS, Kutateladze 18, Novosibirsk 128, 630128 Russia, [b]Novosibirsk State University, Pirogova 2, Novosibirsk 90, 630090 Russia, and [c]University of Marburg, Departments of Mineralogy and of Physical Chemistry, Center of Material Sciences, Hans-Meerwein Strasse, 35032 Marburg/Lahn, Germany

Correspondence e-mail: elena@solid.nsk.su

Received 29 September 1999
Accepted 25 October 1999

The anisotropy of structural distortion of the monoclinic polymorph of acetaminophen induced by hydrostatic pressure up to 4.0 GPa was studied by single-crystal X-ray diffraction in a Merrill–Bassett diamond anvil cell (DAC). The space group ($P2_1/n$) and the general structural pattern remained unchanged with pressure. Despite the overall decrease in the molar volume with pressure, the structure expanded in particular crystallographic directions. One of the linear cell parameters (c) passed through a minimum as the pressure increased. The intramolecular bond lengths changed only slightly with pressure, but the changes in the dihedral and torsion angles were very large. The compressibility of the intermolecular hydrogen bonds NH$\cdots$O and OH$\cdots$O was measured. NH$\cdots$O bonds were shown to be slightly more compressible than OH$\cdots$O bonds. The anisotropy of structural distortion was analysed in detail in relation to the pressure-induced changes in the molecular conformations, to the compression of the hydrogen-bond network, and to the changes in the orientation of molecules with respect to each other in the pleated sheets in the structure. Dirichlet domains were calculated in order to analyse the relative shifts of the centroids of the hydrogen-bonded cycles and of the centroids of the benzene rings with pressure.

1. Introduction

4-Hydroxyacetanilide was first prepared by Morse in 1878. Under the names paracetamol, acetaminophen and panadol (Merck Index, 1976) it is now used as an analgesic and antipyretic drug (Grant & Chow, 1991) and is considered to be the most prominent pain-relieving drug among acetanilide derivatives. It is a typical representative of organic drug substances composed of aromatic polyfunctional molecules (Shekunov *et al.*, 1996). Its physical and chemical properties are being intensively studied, such that many papers devoted to various properties of acetaminophen are published every year.

Hydrogen bonding is a primary feature in the crystal structure of acetaminophen. There are two proton donors (NH, OH) within the molecule, and two proton acceptors (C═O, OH). Calculations using the computer program *HABIT* (Clydesdale *et al.*, 1991, 1996) have shown the OH$\cdots$O hydrogen bond to have an energy of -24.12 kJ mol^{-1}, and the weaker NH$\cdots$O hydrogen bond to have an energy of -10.68 kJ mol^{-1}. According to the model calculations the total hydrogen-bonding component in the monoclinic polymorph is equal to 34.79 kJ mol^{-1}, which is approximately 30% of the total lattice energy, *i.e.* a significant component (Hendriksen *et al.*, 1998).

Table 1
Crystal data.

Formula	$C_8H_9NO_2$			
M_r	151.6			
Crystal system	Monoclinic			
Space group	$P2_1/n$			
Z	4			
Radiation	Mo $K\alpha$, $\lambda = 0.71073$ Å			
Pressure (GPa)	1.0	2.0	3.0	4.0
a (Å)	6.9800 (10)	6.8850 (10)	6.8200 (10)	6.6250 (10)
b (Å)	8.915 (2)	8.5819 (7)	8.3740 (10)	7.985 (2)
c (Å)	11.566 (2)	11.5190 (10)	11.5590 (10)	11.916 (2)
β (°)	98.54 (3)	99.120 (10)	99.320 (10)	99.41 (3)
V (Å)^3	711.7 (2)	672.01 (13)	651.43 (14)	621.9 (2)
N reflections for parameters	12 in 8 positions each	12 in 8 positions each	15 in 8 positions each	15 in 8 positions each
θ_{min} for parameters (°)	2.76	2.95	2.96	3.06
θ_{max} for parameters (°)	8.70	9.01	9.08	9.38
D_x (Mg m^{-3})	1.411	1.494	1.541	1.615
μ (mm^{-1})	0.102	0.108	0.112	0.117

Table 2
Data collection.

Equipment	MB diamond anvil cell; STOE four-circle diffractometer			
Data-collection procedure	Fixed-φ mode; ω-scans			
Absorption by the DAC correction	Experimentally measured curve for the empty DAC			
Be background	Suppressed by a special collimator			
2 standard reflections ($0\bar{2}\bar{2}$, $0\bar{2}2$) every 3 h				
No intensity decay				
100 points per reflection, step 0.01°, 5 s per point				
Pressure (GPa)	1.0	2.0	3.0	4.0
N reflections (measured)	2585	2167	2084	2008
N reflections (independent)	627	613	601	581
N reflections with $I > 2\sigma(I)$	328	360	364	351
R_{int}	0.0490	0.0668	0.0509	0.0472
θ_{max} (°)	27.49	27.49	27.48	27.50
h	$-5 \rightarrow 5$	$-5 \rightarrow 5$	$-5 \rightarrow 5$	$-5 \rightarrow 5$
k	$-11 \rightarrow 11$	$-11 \rightarrow 11$	$-10 \rightarrow 10$	$-10 \rightarrow 10$
l	$-14 \rightarrow 14$	$-13 \rightarrow 13$	$-13 \rightarrow 13$	$-14 \rightarrow 14$

Table 3
Structure refinement.

Refinement on F^2				
Non H-atoms refinement	Anisotropic			
H-atom refinement	Isotropic			
Scattering factors	*International Tables for Crystallography* (1992, Vol. C)			
Pressure (GPa)	1.0	2.0	3.0	4.0
R [$F^2 > 2\sigma(F^2)$]	0.0352	0.0325	0.0308	0.0312
R [F^2], all	0.1002	0.0859	0.08150	0.0810
$wR(F^2)$	0.0532	0.0546	0.0481	0.0632
S	0.838	0.919	0.803	0.893
N reflections	627	613	601	581
N parameters	113	113	113	113
Extinction coefficient	0.014 (3)	0.0080 (15)	0.0119 (13)	0.012 (2)
$(\Delta/\sigma)_{max}$	<0.001	<0.001	<0.001	<0.001
$\Delta\rho_{max}$ (e Å^{-3})	0.103	0.105	0.099	0.117
$\Delta\rho_{min}$ (e Å^{-3})	−0.074	−0.100	−0.101	−0.109

Additives disrupting hydrogen bonding in crystals of acetaminophen were shown to lead to significant changes in the energetics involved and thus alter the morphology and crystallization characteristics of this compound (Hendriksen *et al.*, 1998). Hydrogen bonds were reported to play an important role in defining the anisotropy of the sublimation of different faces of acetaminophen crystals, as well as the anisotropy of the dissolution of different faces in the same solvent and of the same face in different solvents (Vasilchenko *et al.*, 1996, 1997; Boldyrev *et al.*, 1997*a*,*b*). The relative stability/metastability and the crystallization conditions of the three polymorphs of acetaminophen (Haisa *et al.*, 1974, 1976; Di Martino *et al.*, 1997; Nichols & Frampton, 1998) can also be controlled by interacting with the hydrogen-bond networks in the structures. For example, the orthorhombic polymorph II can be stabilized by binding acetaminophen to the selected inorganic supports which are able to participate in hydrogen-bond formation (Politov, Vasilchenko & Boldyrev, unpublished results).

Intermolecular interactions in crystals, in particular hydrogen bonds, manifest themselves in the response of structures to changes in temperature or pressure. More often one is interested in phase transitions induced by these actions. At the same time a study of the anisotropy of a continuous structural distortion in the temperature and pressure range where no phase transitions take place can give valuable information on the intermolecular interactions. These studies may be helpful to understand the role of hydrogen bonds in the cooperative processes of structural distortion resulting from external actions, or due to a phase transition or

chemical reaction in the solid. Variable-pressure studies are less common than variable-temperature studies, probably because high-pressure diffraction experiments are more difficult. However, it is possible to achieve much larger structural distortions in molecular crystals when applying pressure than when changing temperature, and this is important for studying relatively weak intermolecular interactions. It is especially informative to compare the high-pressure behaviour of different polymorphs of the same compound or of related compounds (Katrusiak & Nelmes, 1986; Katrusiak, 1990, 1991*a*,*b*,*c*, 1995; Boldyreva, 1994, 1996, 1999; Boldyreva *et al.*, 1994, 1997*a*,*b*, 1998*a*,*b*).

A study of the pressure-induced changes in cell parameters of the monoclinic polymorph of acetaminophen was carried out in a comparison with those in phenacetin (Shakhtshneider *et al.*, 1998, 1999). Qualitative differences in the anisotropy of lattice compression of the two structures were observed. The structure of phenacetin compressed in all directions. The structure of acetaminophen expanded in several directions with increasing pressure, despite a decrease in the overall volume (Shakhtshneider *et al.*, 1998, 1999). The difference in behaviour of the two structures under pressure was supposed to be due to the different hydrogen-bond networks. In order to test this hypothesis a full structural analysis based on the data of the pressure-induced changes, not only of lattice parameters but also of the atomic coordinates, was required. The present contribution reports on the details of such an analysis for the monoclinic polymorph of acetaminophen.

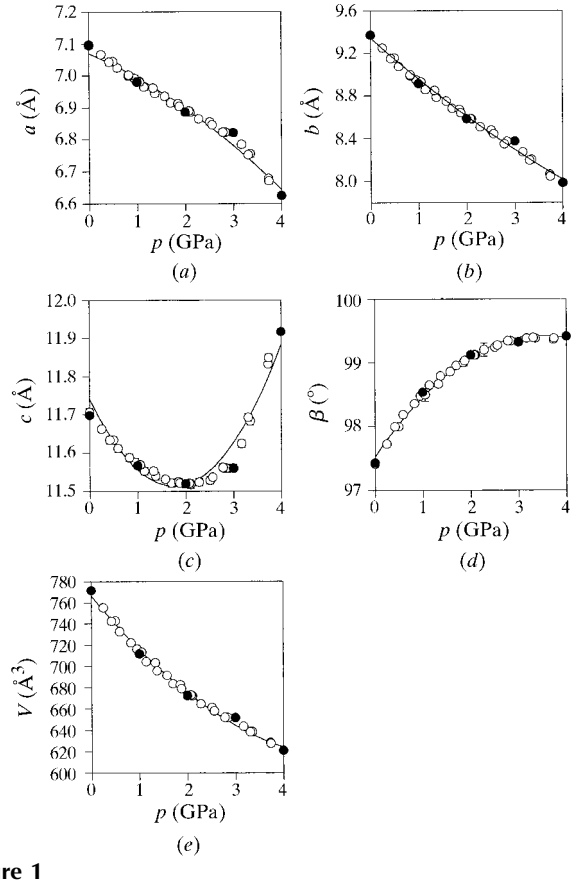

Figure 1
The changes in cell parameters (*a*) *a*, (*b*) *b*, (*c*) *c*, (*d*) β and (*e*) volume of the monoclinic polymorph of acetaminophen with pressure. Black points correspond to the pressure values at which full structure refinements were carried out. The curves are guides to the eye.

2. Experimental

Commercially available acetaminophen produced at Kursk Pharmaceutical Plant, Russia, was used. A single crystal of the monoclinic polymorph of this compound (0.25 mm in diameter and 0.07 mm thick) was grown at ambient temperature from ethanol–water (1:1) solution by slow evaporation under an optical microscope.

The pressure was created in a Merrill–Bassett diamond anvil cell (DAC; Merrill & Bassett, 1974) of the four-screw type suggested by Mao & Bell (1980); the cell has been described by Ahsbahs *et al.* (1993). A pentane–isopentane (1:1) mixture was used as an inert pressure-transmitting liquid. Ruby fluorescence (Piermarini *et al.*, 1975) was used for pressure measurement with an accuracy of 0.05 GPa.

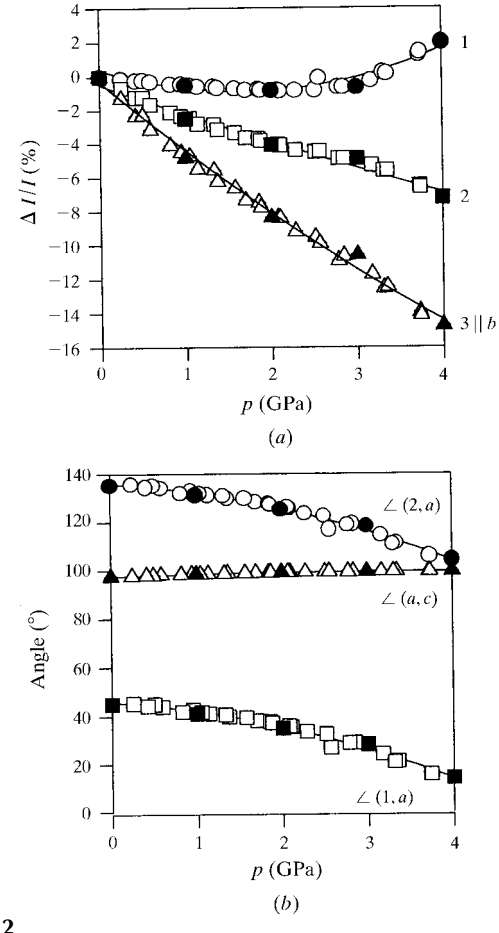

Figure 2
Linear strain in the directions of the principle axes of the strain ellipsoid (*a*) and the angles of the principle axes of the strain ellipsoid with the crystallographic axes (*b*) for pressure-induced structural distortion of the monoclinic polymorph of acetaminophen. Axis 3 (maximum compression) of the strain ellipsoid coincides with the crystallographic axis *b*. Axes 1 and 2 are in the (*ac*)-plane. For comparison, the change in the angle between the *a* and *c* axes with pressure is also plotted. Black points correspond to the pressure values at which full structure refinements were carried out. The curves are guides to the eye.

The crystal was oriented in the DAC in such a way that the (001) face was normal to the beam. The crystal was glued to one of the diamond culets with epoxy glue. The diameter of the diamond culet was 0.6 mm. A hole of diameter 0.45 mm was drilled into the gasket (steel 220.0250/R/l) by spark-erosion technique (Ahsbahs, 1984). The size of the hole allowed the collection of diffraction data in the angle ranges for ω and $(2\theta - \omega)$ up to 40°. The crystal was centred on the diffractometer visually in two directions. Centring in the third direction (direction of the primary beam coinciding with the direction of the DAC axis) was performed according to the method of Ahsbahs, described by Sowa (1994) and by Boldyreva, Ahsbahs *et al.* (1998).

Diffraction experiments were carried out using a Stoe four-circle diffractometer with the software specially adapted for high-pressure data collection (Kutoglu, 1997). Mo $K\alpha$ radiation (λ = 0.71073 Å) and a graphite monochromator were used. A special procedure was applied for the lattice parameter measurements (Hazen & Finger, 1982; Kutoglu, 1997) so that each reflection was measured in eight positions. Comparative studies at all the pressures were carried out for the same crystal in the same orientation in the DAC. The reflections remained sharp at high pressures. The crystal remained unchanged after being stored in the DAC at high pressure; it returned to the initial state after the DAC was unloaded back to ambient pressure.

To minimize the absorption of the X-rays by the DAC the fixed-φ method (Finger & King, 1978; Kutoglu, 1997) was applied for data collection. The absorption of the X-rays by the empty DAC was measured experimentally and the results were used to correct the intensities of the reflections (Finger & King, 1978; Ahsbahs, 1987). Since the background was 2θ-dependent, ω-scans were used for data collection (Ahsbahs, 1987). The Be background was entirely suppressed by the use of an edge-shaped collimator in front of the detector, as described by Ahsbahs (1987). This allowed up to fourfold improvement of the signal-to-background ratio (Ahsbahs, 1987). To improve this ratio further the size of the counter

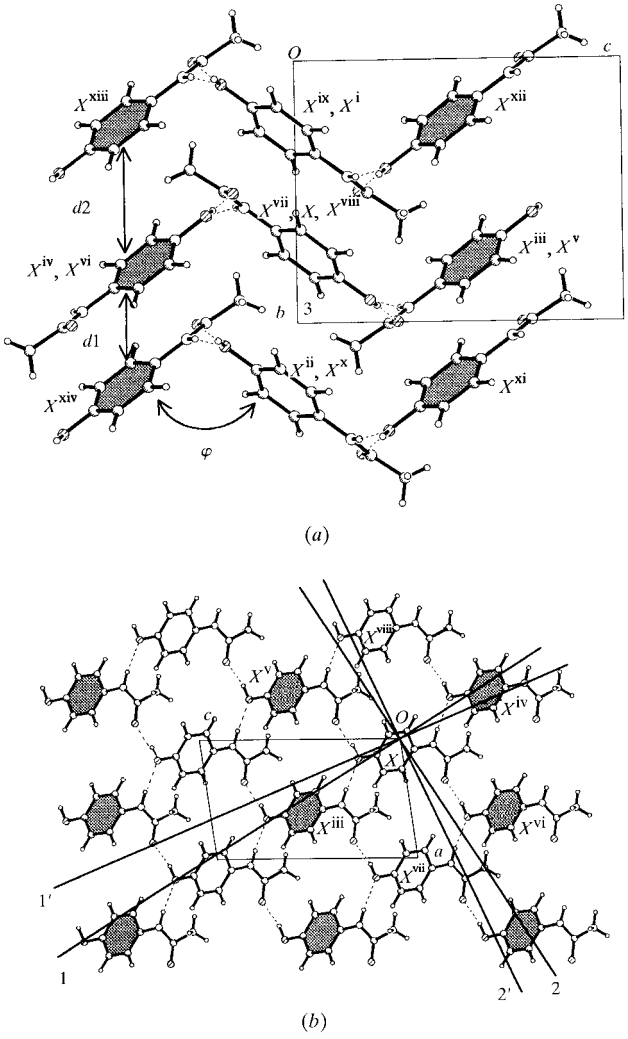

Figure 3
Directions of the principle axes 3 (*a*) and 1 and 2 (*b*) of the strain ellipsoid with respect to the fragments of the crystal structure of the monoclinic polymorph of acetaminophen. 1, 2 – axes at pressure p = 1.0 GPa; 1′, 2′ – axes at p = 4.0 GPa. The unit cell and the crystallographic axes are also shown. Dashed lines indicate hydrogen bonds in the structure. Symmetry codes of the benzene rings centroids *X*: (i) $-x, -y+1, -z$; (ii) $-x, -y+2, -z$; (iii) $x+\frac{1}{2}, -y+\frac{3}{2}, z+\frac{1}{2}$; (iv) $x-\frac{1}{2}, -y+\frac{3}{2}, z-\frac{1}{2}$; (v) $x-\frac{1}{2}, -y+\frac{3}{2}, z+\frac{1}{2}$; (vi) $x+\frac{1}{2}, -y+\frac{3}{2}, z-\frac{1}{2}$; (vii) $x+1, y, z$; (viii) $x-1, y, z$; (ix) $-x+1, -y+1, -z$; (x) $-x+1, -y+2, -z$; (xi) $-x+\frac{1}{2}, y+\frac{1}{2}, -z+\frac{1}{2}$; (xii) $-x+\frac{1}{2}, y-\frac{1}{2}, -z+\frac{1}{2}$; (xiii) $-x+\frac{1}{2}, y-\frac{1}{2}, -z-\frac{1}{2}$; (xiv) $-x+\frac{1}{2}, y+\frac{1}{2}, -z-\frac{1}{2}$. The shaded benzene rings are parallel to each other, the unshaded benzene rings are orthogonal. The distances of the benzene ring centroids from the projection (*bc*)-plane (Å) are (*a*) 0.799 (2) (*X*), −0.799 (2) (X^{i}, X^{ii}), 4.316 (2) (X^{iii}, X^{vi}), −2.718 (2) (X^{iv}, X^{v}), 7.833 (2) (X^{vii}), −6.235 (2) (X^{viii}), 6.235 (2) (X^{ix}, X^{x}), 2.718 (2) (X^{xi}, X^{xii}, X^{xiii}, X^{xiv}). The distances of the benzene ring centroids from the projection (*ac*)-plane (Å) are (*b*) 7.166 (2) (X^{iii}, X^{iv}, X^{v}, X^{vi}), 6.885 (2) (*X*, X^{vii}, X^{viii}).

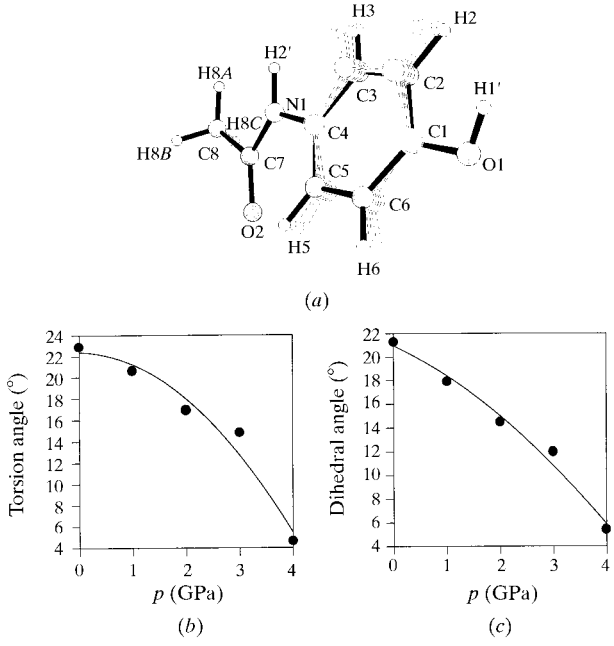

Figure 4
The intramolecular changes in acetaminophen with pressure. (*a*) A general view of a molecule at different pressures. (*b*) Torsion angle C3—C4—N1—C7 *versus* pressure. (*c*) Dihedral angle δ between the planes C1—C2—C3—C4—C5—C6 and N1—C7—O2—C8 *versus* pressure. The curves are guides to the eye.

aperture in 2θ and χ was varied with 2θ. The data were collected in the full reciprocal volume allowed by the shadow from the DAC [ω in the range from -39 to 40°, χ in the range from -86 to 96°, 2θ in the range from 3 to 55°, $(2\theta - \omega)$ in the range from -39 to 40° at $\varphi = \varphi_0$ and $\varphi = \varphi_0 + 180^\circ$; this gave $\sim$30–40% of the total number of reflections, which could be measured without the DAC]. The equivalent reflections were merged. In order to gain as good a signal-to-background ratio and as many observable reflections as possible, the data collection was very slow (4–6 s per point, 100 points per reflection, with 0.01° per step). All the reflections were collected in the full-profile mode. The raw diffraction data were processed using the computer program *PROFILE* (Naumov & Boldyreva, 1997). *SHELXL*97 (Sheldrick, 1997) was used for structure refinement. *CAVITY* (Naumov & Boldyreva, 1999) was used for plotting the fragments of crystal structures and for calculating distances and angles in the structures. Strain tensors were calculated using Ohashi's program *TENSOR*, published in the book by Hazen & Finger (1982). *NADI* was applied for calculating Dirichlet domains (Kashcheeva *et al.*, 1999).

Crystal data, details on the data collection and on the structure refinement are summarized in Tables 1–3.

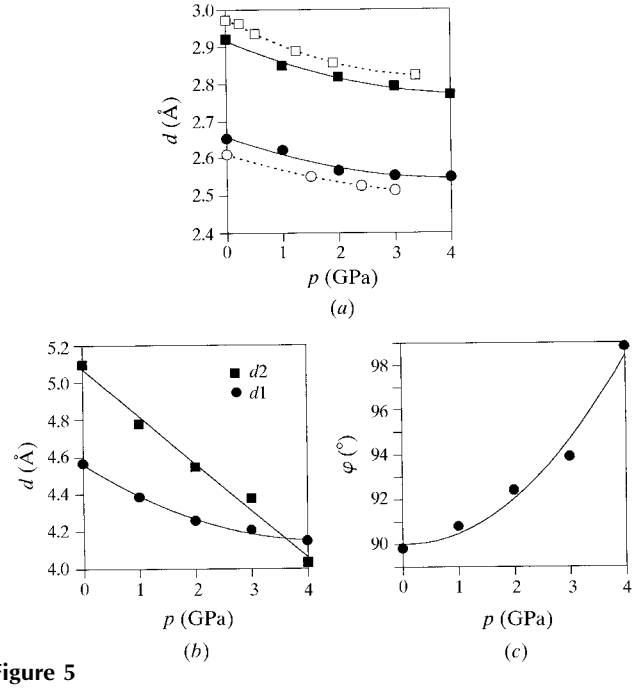

Figure 5
The changes in the intermolecular contacts in acetaminophen with pressure. (*a*) Distances between non-H atoms in the NH$\cdots$O (filled squares) and OH$\cdots$O (filled circles) hydrogen bonds in the pleated layers. The dashed lines show, for comparison, the data on pressure-dependence of N(H)$\cdots$O (empty squares) distances in $[Co(NH_3)_5NO_2]Cl_2$ (Boldyreva *et al.*, 1998*a*) and of the O(H)$\cdots$O (empty circles) distances in 2-methyl-1,3-cyclopentanedione (Katrusiak, 1991*a*). (*b*) Distances between the molecules belonging to different pleated layers (see also Fig. 3*a*). (*c*) Angles between the planes of the neighbouring benzene rings of the molecules belonging to the same pleated layer, defined as the angle between the normals to the intersection line of the planes (see also Fig. 3*a*). The errors do not exceed the size of the symbols. The curves are guides to the eye.

3. Results and discussion

The changes in cell parameters and volume with pressure are plotted in Fig. 1. One of the linear lattice parameters (c) passed through a minimum as the pressure increased. The measured changes in cell parameters were used to calculate the strain tensor. Linear strain along the directions of the principle axes of the strain ellipsoid and the angles of these principle axes with the crystallographic axes of the structure are plotted in Fig. 2.

The acetaminophen molecules in the monoclinic polymorph are linked by a hydrogen-bond network formed by OH$\cdots$O and NH$\cdots$O hydrogen bonds in pleated layers {010}. The sheets are attached along the [010] axis by relatively strong interactions between the benzene rings (Fig. 3). These three types of interactions contribute $\sim$60% of the entire lattice energy and define the anisotropy of the crystal properties (Shekunov *et al.*, 1996). The main compression of the structure (principle axis 3) was observed in the direction of crystallographic axis b, normal to the pleated sheets formed by acetaminophen molecules (Figs. 2*a* and 3*a*). Despite the overall decrease in molar volume with pressure, the structure expanded in particular crystallographic directions, the effect being pronounced at pressures higher than 3.0 GPa. The largest expansion was observed in the direction of axis 1 of the strain ellipsoid in the (ac)-plane (Figs. 2*a* and 3*b*). With increasing pressure the principle axes 1 and 2 of the strain ellipsoid rotated in the (ac)-plane with respect to crystallographic axes a and c of the structure (Figs. 2*b* and 3*b*).

At all the pressures the structure could be refined in the same space group ($P2_1/n$). The slight kinks of the $V(P)$, $a(P)$ and $b(P)$ curves in the range between 3.0 and 4.0 GPa might indicate a phase transition (into a phase very closely structurally related to the original one, probably isosymmetrical); a detailed further study with complementary techniques (calorimetry, inelastic scattering, Raman spectroscopy) would be required in order to test this. The pressure-induced changes in the atomic coordinates and in the atomic displacement parameters were followed. Fractional coordinates and the equivalent isotropic displacement parameters for non-H atoms are summarized in Table 4. Anisotropic displacement parameters and the H-atom coordinates are deposited.[1] Numeration of atoms and connectivity are explained in Fig. 4(*a*).

The intramolecular bond lengths in the acetaminophen molecules almost did not change with increasing pressure. A slight elongation of the C=O bond (0.023 Å at 4.0 GPa) was measured, which was in good agreement with the data previously reported by Katrusiak (1991*b*,*c*) for 2-methyl-1,3-cyclopentanedione (0.02 Å at 3.01 GPa) and correlated well with the pressure-induced shortening of the OH$\cdots$O hydrogen bonds (see below). The value of the N1—C7—C8 angle increased by 3° at 4.0 GPa. Much more pronounced changes were observed with pressure for the torsion angle

[1] Supplementary data for this paper are available from the IUCr electronic archives (Reference: AV0025). Services for accessing these data are described at the back of the journal.

Table 4
Fractional atomic coordinates and equivalent isotropic dispacement parameters (Å^2) of non H-atoms at 1.0, 2.0, 3.0 and 4.0 GPa (1st, 2nd, 3rd, 4th lines downwards).

$$U_{eq} = (1/3)\Sigma_i\Sigma_j U^{ij} a^i a^j \mathbf{a}_i.\mathbf{a}_j.$$

	x	y	z	U_{eq}
O1	0.1594 (6)	0.9332 (2)	0.2213 (3)	0.050 (3)
	0.1537 (5)	0.9479 (2)	0.2216 (2)	0.039 (2)
	0.1501 (5)	0.95610 (18)	0.2223 (2)	0.037 (2)
	0.1447 (5)	0.9750 (2)	0.2205 (2)	0.033 (3)
C1	0.1298 (8)	0.8364 (3)	0.1280 (3)	0.029 (3)
	0.1228 (7)	0.8456 (3)	0.1292 (3)	0.022 (3)
	0.1206 (6)	0.8513 (2)	0.1294 (2)	0.027 (3)
	0.1148 (8)	0.8669 (3)	0.1292 (3)	0.020 (3)
C2	−0.0470 (7)	0.8305 (2)	0.0547 (3)	0.038 (4)
	−0.0579 (6)	0.8346 (2)	0.0565 (2)	0.025 (3)
	−0.0636 (6)	0.8375 (2)	0.0586 (2)	0.025 (3)
	−0.0785 (7)	0.8444 (3)	0.0648 (2)	0.018 (3)
C3	−0.0652 (8)	0.7338 (3)	−0.0400 (3)	0.031 (3)
	−0.0748 (7)	0.7335 (3)	−0.0381 (3)	0.036 (3)
	−0.0803 (7)	0.7346 (2)	−0.0364 (3)	0.032 (3)
	−0.0967 (8)	0.7377 (3)	−0.0281 (3)	0.027 (3)
C4	0.0824 (7)	0.6436 (3)	−0.0606 (3)	0.023 (4)
	0.0769 (6)	0.6436 (2)	−0.0601 (2)	0.015 (3)
	0.0747 (6)	0.6554 (3)	0.0601 (2)	0.017 (3)
	0.0684 (8)	0.6554 (3)	−0.0552 (3)	0.016 (3)
C5	0.2575 (6)	0.6468 (3)	0.0148 (2)	0.025 (3)
	0.2589 (6)	0.6505 (2)	0.0146 (2)	0.028 (3)
	0.2591 (5)	0.6553 (2)	0.0144 (2)	0.025 (3)
	0.2612 (6)	0.6722 (2)	0.0124 (2)	0.019 (3)
C6	0.2784 (8)	0.7444 (3)	0.1088 (3)	0.032 (3)
	0.2771 (7)	0.7527 (3)	0.1090 (3)	0.019 (3)
	0.2775 (6)	0.7597 (3)	0.1089 (3)	0.019 (2)
	0.2776 (7)	0.7783 (3)	0.1057 (3)	0.021 (3)
N1	0.0475 (9)	0.5488 (3)	−0.1608 (3)	0.032 (4)
	0.0458 (7)	0.5454 (2)	−0.1610 (2)	0.020 (3)
	0.0415 (6)	0.5455 (2)	−0.1610 (2)	0.021 (2)
	0.0344 (7)	0.5533 (3)	−0.1546 (2)	0.024 (3)
C7	0.1765 (12)	0.4814 (4)	−0.2188 (4)	0.024 (4)
	0.1732 (9)	0.4727 (3)	−0.2172 (3)	0.031 (3)
	0.1716 (8)	0.4700 (3)	−0.2146 (3)	0.029 (3)
	0.1673 (9)	0.4686 (3)	−0.2041 (3)	0.027 (4)
O2	0.3515 (7)	0.4873 (2)	−0.1883 (3)	0.047 (3)
	0.3530 (6)	0.4752 (2)	−0.1850 (2)	0.037 (3)
	0.3522 (5)	0.4694 (2)	−0.1808 (2)	0.032 (2)
	0.3534 (6)	0.4672 (2)	−0.1692 (2)	0.031 (2)
C8	0.0868 (9)	0.3948 (3)	−0.3257 (3)	0.057 (4)
	0.0824 (7)	0.3854 (3)	−0.3257 (3)	0.041 (3)
	0.0795 (7)	0.3814 (3)	−0.3234 (2)	0.045 (3)
	0.0812 (8)	0.3730 (3)	−0.3091 (3)	0.035 (3)

C3—C4—N1—C7 (Fig. 4*b*) and the dihedral angle δ between the planes C1—C2—C3—C4—C5—C6 and N1—C7—O2—C8 (Fig. 4*c*), especially in the pressure range 3.0–4.0 GPa. The molecules became noticeably flatter with pressure (mean deviations of all non-H atoms from a common averaged plane being 0.14 Å at ambient pressure and 0.05 Å at 4.0 GPa).

The major changes in the structure with increasing pressure were observed in the intermolecular distances and angles. Most of the intermolecular contacts, including the OH···O and NH···O hydrogen bonds (Fig. 5*a*), and the distances between the molecules belonging to different pleated layers (Fig. 5*b*) shortened noticeably. When H atoms cannot be located very reliably (which is the case when using photographic methods, in protein crystallography or, as in the present paper, in DAC high-pressure studies), the angles between the lines linking the non-H atoms of the molecular

Table 5
Angles between lines linking non-H atoms in the NH···O and OH···O intermolecular hydrogen bonds in the monoclinic polymorph of acetaminophen at different pressures.

Angle	10^{-4} GPa†	1.0 GPa	2.0 GPa	3.0 GPa	4.0 GPa
C1—O1—O2^{i}	116.6	116.5	117.0	118.1	119.8
O1—O2^{i}—C7^{i}	140.7	137.7	135.7	133.1	128.5
C7—N1—O1^{ii}	117.6	116.5	115.6	115.2	110.4
C4—N1—O1^{ii}	112.5	113.0	112.8	114.3	120.0
N1—O1^{ii}—C1^{ii}	116.9	115.6	113.8	112.9	112.0

Symmetry codes: (i) $x-\frac{1}{2}, -y+\frac{3}{2}, z-\frac{1}{2}$; (ii) $x-\frac{1}{2}, -y+\frac{3}{2}, z+\frac{1}{2}$ [equivalent to (iv) and (v) in caption to Fig. 3]. † Data at ambient pressure were obtained for the same crystal in the same DAC.

fragments involved in the hydrogen bonds OH···O and NH···O can be used to characterize the hydrogen bonds (Katrusiak, 1996). The corresponding values for the OH···O and NH···O hydrogen bonds in the monoclinic polymorph of acetaminophen changed considerably with increasing pressure (Table 5). The longer and [according to Hendriksen *et al.* (1998)] weaker NH···O hydrogen bonds in acetaminophen were shown to be slightly more compressible than the OH···O hydrogen bonds. The compressibility of the NH···O hydrogen bonds measured for acetaminophen was comparable with that previously reported for the NH···O hydrogen bonds in $[Co(NH_3)_5NO_2]Cl_2$ (Boldyreva *et al.*, 1998*a*). The compressibility of the OH···O hydrogen bonds in acetaminophen was similar to that measured by Katrusiak (1991*a*) for 2-methyl-1,3-cyclopentanedione.

Shortening of the intermolecular hydrogen bonds with pressure can be interrelated with the observed flattening of the acetaminophen molecules. According to the *ab initio* quantum chemical HF/6-31G calculations (Binev *et al.*, 1998) the dihedral angle between the benzene ring and amide group planes, corresponding to the minimum energy of an individual acetaminophen molecule, is extremely sensitive to the protonation/deprotonation of the OH and NH groups. According to the calculations, in the most stable conformer of an isolated molecule the dihedral angle is 0.3° (the molecule is almost flat). In the isolated oxyanion (deprotonated OH group) the dihedral angle has been calculated to be 90.0°, and in the dianion (also deprotonated NH group) the molecule should

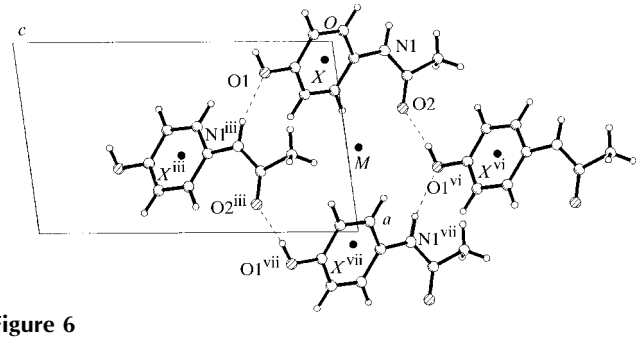

Figure 6
A hydrogen-bonded cycle (a fragment of the two-dimensional network) in the monoclinic polymorph of acetaminophen. For symmetry codes of the benzene ring centroids *X*, see the caption to Fig. 3.

become flat again, with a coplanar phenylene ring and amide group, and the dihedral angle between them being 0.0005°.

In the crystal structure of acetaminophen the dihedral angle is 20–21° (Haisa *et al.*, 1976; Naumov *et al.*, 1998), which results from intermolecular interactions, in particular from the formation of a hydrogen-bond network involving NH···O and OH···O bonds (effective partial deprotonation of the NH and OH groups). As the pressure increases and OH···O and NH···O are shortened, the dihedral angle in the molecules decreases. A flatter shape of the molecule is, at the same time, more favourable for achieving a denser packing.

With increasing pressure the angle between the planes of the benzene rings of the molecules belonging to the same layer changed (Fig. 5*c*). At the same time the angle between the axes of the benzene rings (defined by vectors C1–C4) remained almost unchanged. The whole pleated layers expanded in the direction close to the diagonal between the crystallographic axes *a* and *c* in the (*ac*)-plane due to the relative rotation of the benzene rings of the adjacent molecules and to the changes in the dihedral and torsion angles of the individual molecules.

It is remarkable that, with increasing pressure, hydrogen-bonded pleated sheets of acetaminophen molecules contracted in the direction close to that of the chains linked alternatively by NH···O and OH···O hydrogen bonds, and expanded in that of the NH···O bonded chains (Fig. 3), although both O(H)···O and N(H)···O distances decreased with pressure (Fig. 5*a*). To understand better the observed anisotropy of structural distortion with pressure, it was helpful to consider the hydrogen-bonded cycles (Fig. 6) forming the two-dimensional network in the structure. The cycles are not flat, the mean absolute deviation of atoms forming hydrogen bonds in the cycle (plus the centroids of the two corresponding benzene rings) from the least-squares averaged common plane being ∼0.27 Å at ambient pressure and 0.30 Å at 4.0 GPa. The pressure-induced shifts of individual atoms forming the hydrogen-bonded cycles with respect to the least-square averaged common plane and to the centroid of the cycle (M) were rather large, but the 'flatness' of the cycle as a whole and the mean distances of different atoms from the cycle centroid changed, but only slightly (Figs. 7*a* and *b*). The sum of all the φ_i angles remained practically unchanged (368° at ambient pressure and at 1.0, 2.0 and 3.0 GPa, and 369° at 4.0 GPa), although the values of individual φ_i angles changed by up to 5° (Fig. 7*c*). Despite all the drastic anisotropic changes in the crystal structure with pressure, the hydrogen-bonded cycles preserved their shape and size to a large extent. This may serve as an indication of the highly cooperative nature of the pressure-induced molecular deformations and displacements in the structure of acetaminophen due to the existence of a two-dimensional network of NH···O and OH···O hydrogen bonds.

Relative shifts of the centroids of the hydrogen-

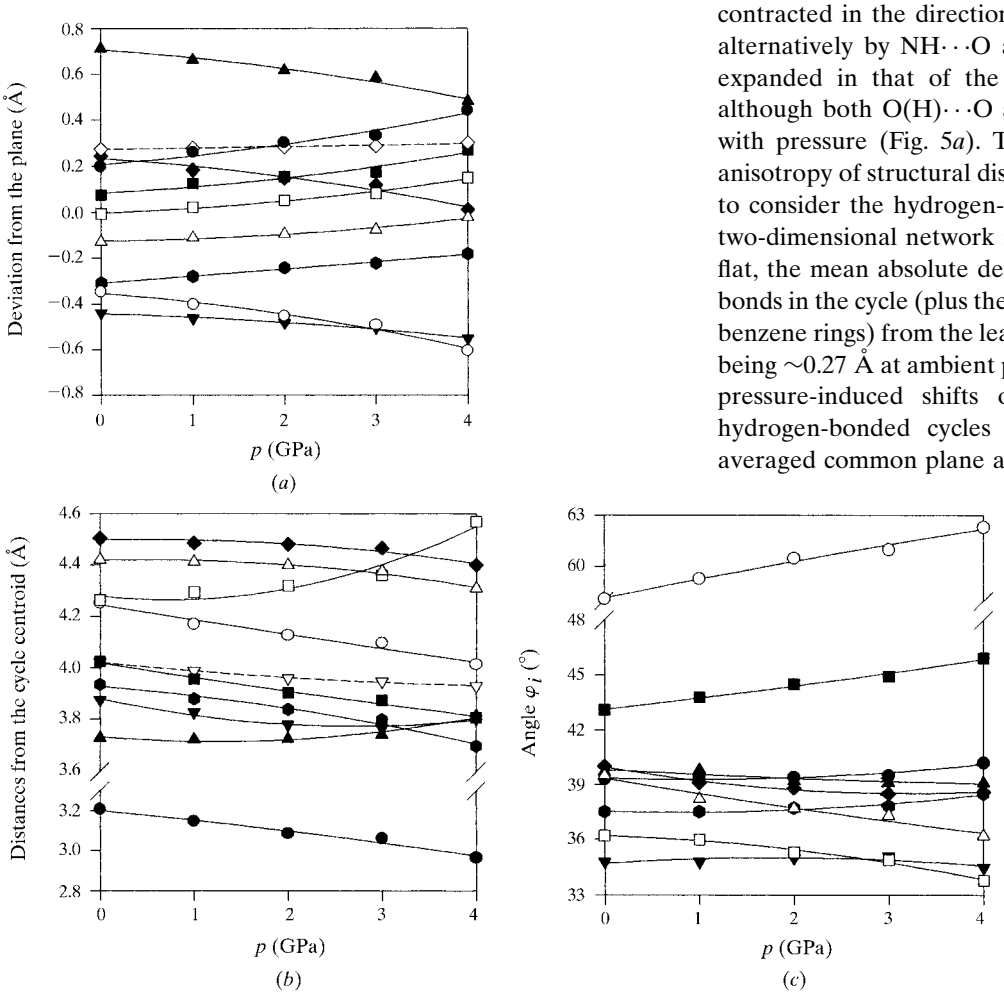

Figure 7
Distortion of hydrogen-bonded cycles (shown in Fig. 6) in the monoclinic polymorph of acetaminophen *versus* pressure. (*a*) Distances of atoms participating in the formation of hydrogen bonds and of the centroids of the benzene rings *X* from the least-squares averaged common plane. Filled triangles, $O1^{vi}$; empty diamonds, average; filled diamonds, $O2^{iii}$; filled circles, O1; filled squares, $O1^{vii}$; empty squares, *X*; empty triangles, X^{vii}; filled hexagons, $N1^{vii}$; empty circles, $N1^{iii}$; filled inverted triangles, O2. (*b*) Their distance to the centroid of the cycle *M*. Filled diamonds, *M*—O1; empty triangles, *M*—$N1^{vii}$; empty squares, *M*—$O1^{vi}$; empty circles, *M*—O2; filled squares, *M*—$O1^{vii}$; empty inverted triangles, average; filled hexagons, *M*—*X*; filled inverted triangles, *M*—$N1^{iii}$; filled triangles, *M*—$O2^{iii}$; filled circles, *M*—X^{vii}. (*c*) The angles between the vectors connecting the centroid of the cycle *M* with the atoms forming the cycle and benzene ring centroids. Empty circles, *X*—*M*—O2; filled squares, $X1^{vii}$—*M*—$O1^{vii}$; filled diamonds, $N1^{iii}$—*M*—O1; filled triangles, $O1^{vii}$—*M*—$O2^{iii}$; empty triangles, $O1^{vi}$—*M*—$N1^{vii}$; filled circles, $N1^{vii}$—*M*—X^{vii}; filled hexagons, O1—*M*—*X*; empty squares, O2—*M*—$O1^{vi}$; filled inverted triangles, $O2^{iii}$—*M*—$N1^{iii}$. Symmetry codes of the centroids of the benzene rings are given in the caption to Fig. 3. Symmetry codes of the atoms involved in the hydrogen-bond formation: (iii) $x+\frac{1}{2}$, $-y+\frac{3}{2}$, $z+\frac{1}{2}$; (vii) $x+1$, y, z; (vi) $x+\frac{1}{2}$, $-y+\frac{3}{2}$, $z-\frac{1}{2}$. Dashed lines: average absolute deviations from the plane (*a*) and the average distance to the centroid of the cycle (*b*) *versus* pressure. The curves are guides to the eye.

bonded cycles with respect to each other could be most clearly followed by calculating their corresponding Dirichlet domains (DD) at different pressures (Figs. 8 and 9). The shape of the DD was to a large extent preserved with pressure, and the evolution of relative face areas was continuous.

The changes in the relative face areas of the DD with increasing pressure are a manifestation of the changes in the contributions of the centroids of the different hydrogen-bonded cycles to the coordination of the cycle which was chosen as the central one (Fig. 9). The relative areas of the two larger faces (1 and 2) grow even more with increasing pressure, and this corresponds to the major contraction of the structure along the *b* axis. A complex interplay in the relative areas of other faces is a manifestation of the anisotropic compression/expansion of the structure. At all the pressures the number of faces of a DD remained equal to 14; whereas the two smallest faces (13 and 14) disappeared with pressure and two new small faces (15 and 16) appeared instead.

Compression of the hydrogen-bond network is interrelated with the rotation of benzene rings in the individual molecules, which increases the packing density at higher pressures and decreases steric hindrances between particular molecular fragments.

Pressure-induced compression of hydrogen bonds and rotation of benzene rings resulted in shifts of the centroids of the benzene rings with respect to each other. Thus, two centroids of the benzene rings of the molecules forming a hydrogen-bonded cycle (X and X^{vii}) approached the centroid of this cycle M (coming $\sim$0.2 Å closer by 4.0 GPa than at ambient pressure), whereas the distances from the cycle centroid M to the two other benzene rings centroids (X^{iii} and X^{vi}) increased (becoming $\sim$0.1–0.15 Å longer by 4.0 GPa), which is in good agreement with the expansion of the structure in the direction of axis 1 and of its medium contraction along the axis 2 of the strain ellipsoid.

The relative shifts of the centroids of the benzene rings with pressure were analyzed by calculating the corresponding Dirichlet domains (Figs. 10 and 11). With increasing pressure the largest relative face areas of the DD [corresponding to the centroids of the rings 1 (X^{i}) and 2 (X^{ii})] noticeably increased further, especially that of centroid (2). Both rings 1 and 2 are parallel to the central ring and are located above and below it (at ambient pressure at 4.87 and 4.49 Å, respectively). With increasing pressure up to 3.0 GPa the distances between the central ring and rings 1 and 2 became more and more equal, and at higher pressures seemed to start deviating again. The pronounced changes with pressure in the relative areas of the faces 1 and 2 of the Dirichlet domain are in good agreement with the major compression of the structure along the *b* axis.

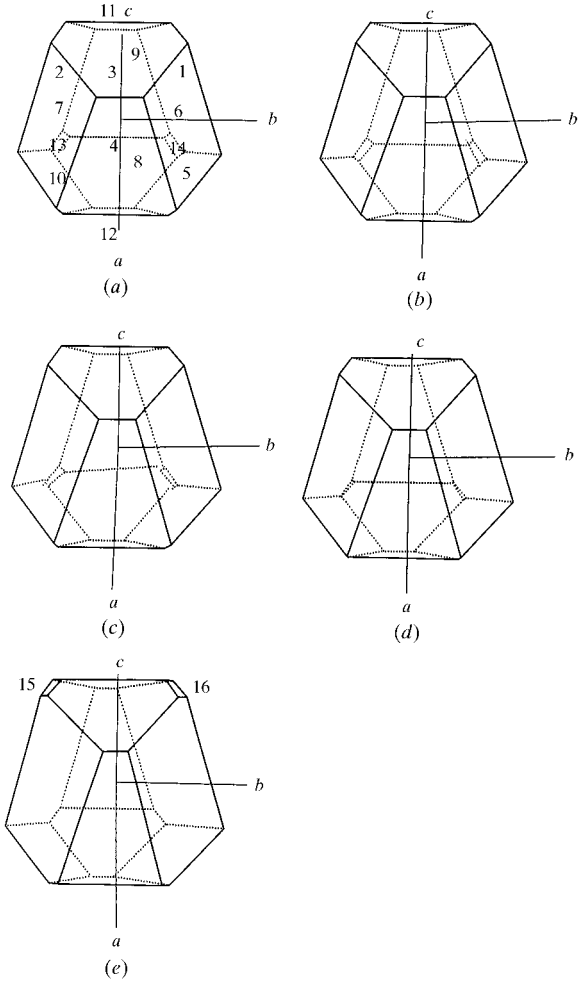

Figure 8
The shape of the Dirichlet domains calculated for the centroids *M* of the hydrogen-bonded cycles (shown in Fig. 6) at (*a*) ambient pressure, (*b*) 1.0 GPa, (*c*) 2.0 GPa, (*d*) 3.0 GPa and (*e*) 4.0 GPa. Numeration of faces corresponds to that in Fig. 9.

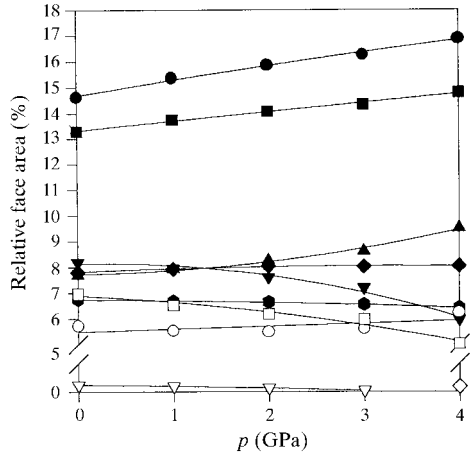

Figure 9
Relative face areas of the Dirichlet domains calculated for the centroids *M* of the hydrogen-bonded cycles (shown in Fig. 6) *versus* pressure. Symmetry codes of centroids corresponding to faces (1) $-x+1, -y+2, -z$; (2) $-x+1, -y+1, -z$; (3) $x-\frac{1}{2}, -y+\frac{3}{2}, z-\frac{1}{2}$; (4) $x+\frac{1}{2}, -y+\frac{3}{2}, z+\frac{1}{2}$; (5) $-x+2, -y+2, -z$; (6) $-x+\frac{3}{2}, y+\frac{1}{2}, -z+\frac{1}{2}$; (7) $-x+\frac{3}{2}, y-\frac{1}{2}, -z+\frac{1}{2}$; (8) $x+\frac{1}{2}, -y+\frac{3}{2}, z-\frac{1}{2}$; (9) $x-\frac{1}{2}, -y+\frac{3}{2}, z+\frac{1}{2}$; (10) $-x+2, -y+1, -z$; (11) $x-1, y, z$; (12) $x+1, y, z$; (13) $-x+\frac{3}{2}, y-\frac{1}{2}, -z-\frac{1}{2}$; (14) $-x+\frac{3}{2}, y+\frac{1}{2}, -z-\frac{1}{2}$; (15) $-x+\frac{1}{2}, y-\frac{1}{2}, -z+\frac{1}{2}$; (16) $-x+\frac{1}{2}, y+\frac{1}{2}, -z+\frac{1}{2}$. Filled circles, 1; filled squares, 2; filled inverted triangles, 3, 4; filled diamonds, 5; filled triangles, 6, 7; empty squares, 8, 9; filled hexagons, 10; empty circles, 11, 12; empty inverted triangles, 13, 14; empty diamonds, 15, 16. Numeration of faces corresponds to that in Fig. 8. The curves are guides to the eye.

It was more difficult to give a simple interpretation of the pressure-induced changes in the relative areas of other faces.

Faces 3 (X^{iii}), 4 (X^{iv}), 5 (X^{v}), 6 (X^{vi}), 11 (X^{xi}), 12 (X^{xii}), 13 (X^{xiii}) and 14 (X^{xiv}) correspond to the rings normal to the central one, whereas rings 7 (X^{vii}), 8 (X^{viii}), 9 (X^{ix}) and 10 (X^{x}) are parallel to the central ring. The molecule with ring centroid 4 (X^{iv}) forms an NH$\cdots$O hydrogen bond with the NH group of the central molecule, the molecule with ring centroid 6 (X^{vi}) forms an OH$\cdots$O hydrogen bond with the C=O fragment of the central molecule, the molecule with ring centroid 5 (X^{v}) forms an OH$\cdots$O hydrogen bond with the OH group of the central molecule, and the molecule with ring centroid 3 (X^{iii}) forms an NH$\cdots$O hydrogen bond with the OH group of the central molecule. Molecules with ring centroids 7 (X^{vii}) and 8 (X^{viii}) do not form any hydrogen bonds with the central molecule directly, but they are involved in the hydrogen-bonded cycles with the central molecule and molecules with ring centroids 3 (X^{iii}), 6 (X^{vi}) and 4 (X^{iv}), 5 (X^{v}), respectively.

The relative areas of faces 3 (4) and 7 (8) became equal at a pressure of 4.0 GPa. The relative areas of faces 7 (8) and 11 (12) increased with increasing pressure. As in the case of the DD of the centroids of the hydrogen-bonded cycles, the total number of faces of a DD for centroids of benzene rings remained equal to 14 at all pressures; as the two smallest faces [13 (X^{xiii}) and 14 (X^{xiv})] disappeared, two new ones [15 (X^{xv}) and 16 (X^{xvi})] appeared.

As complicated as the relative movements of the benzene ring centroids with increasing pressure are, the observed changes are interrelated with the anisotropic cooperative compression of a hydrogen-bond network and the changes in the angles within and between the molecules in the structure.

4. Conclusions

The present study has revealed an anisotropic structural distortion of the monoclinic polymorph of acetaminophen with increasing pressure. The hydrogen-bond network was shown to play a major role in determining directions of major and minor structural compression, and also those of expansion with increasing pressure. The interactions in this network are highly cooperative. At the same time, acetaminophen molecules are flexible with respect to the rotations of the benzene ring relative to the acetanilide group. These two factors account for the rotations of the fragments of acetaminophen molecules with respect to each other.

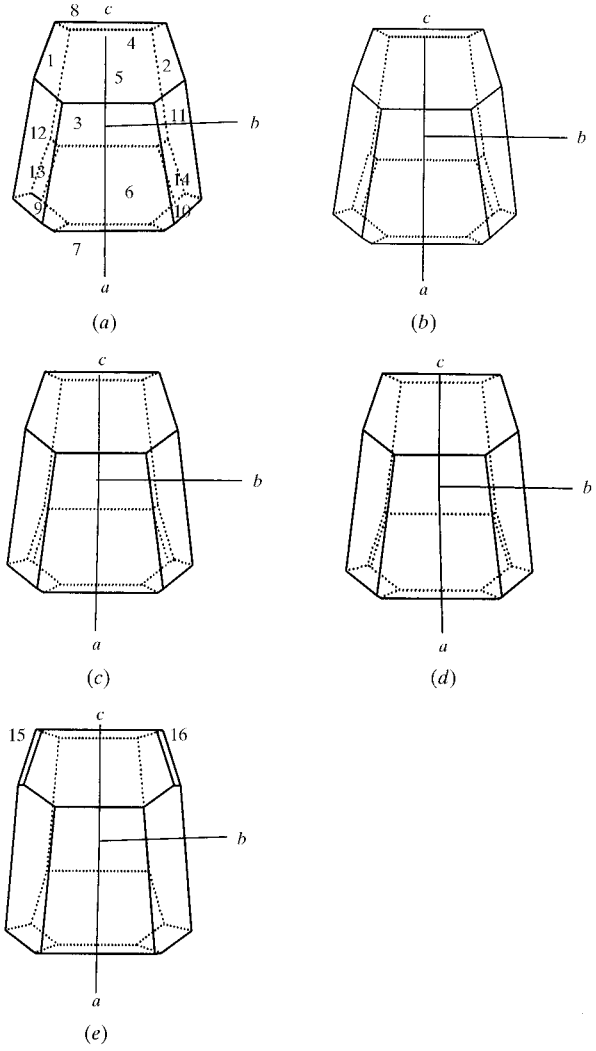

Figure 10
The shape of the Dirichlet domains calculated for the centroids of the benzene rings of acetaminophen molecules in the monoclinic polymorph at (*a*) ambient pressure, (*b*) 1.0 GPa, (*c*) 2.0 GPa, (*d*) 3.0 GPa and (*e*) 4.0 GPa. Numeration of faces corresponds to that in Fig. 11.

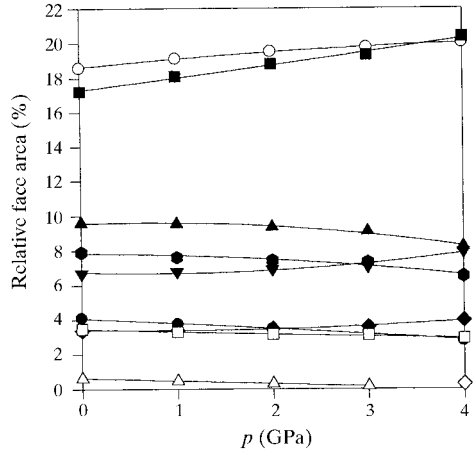

Figure 11
Relative face areas of the Dirichlet domains calculated for the centroids of the benzene rings of acetaminophen molecules in the monoclinic polymorph *versus* pressure. Symmetry codes of centroids corresponding to faces (1) $-x, -y+1, -z$; (2) $-x, -y+2, -z$; (3) $x+\frac{1}{2}, -y+\frac{3}{2}, z+\frac{1}{2}$; (4) $x-\frac{1}{2}, -y+\frac{3}{2}, z-\frac{1}{2}$; (5) $x-\frac{1}{2}, -y+\frac{3}{2}, z+\frac{1}{2}$; (6) $x+\frac{1}{2}, -y+\frac{3}{2}, z-\frac{1}{2}$; (7) $x+1, y, z$; (8) $x-1, y, z$; (9) $-x+1, -y+1, -z$; (10) $-x+1, -y+2, -z$; (11) $-x+\frac{1}{2}, y+\frac{1}{2}, -z+\frac{1}{2}$; (12) $-x+\frac{1}{2}, y-\frac{1}{2}, -z+\frac{1}{2}$; (13) $-x+\frac{1}{2}, y-\frac{1}{2}, -z-\frac{1}{2}$; (14) $-x+\frac{1}{2}, y+\frac{1}{2}, -z-\frac{1}{2}$; (15) $-x-\frac{1}{2}, y-\frac{1}{2}, -z+\frac{1}{2}$; (16) $-x-\frac{1}{2}, y+\frac{1}{2}, -z+\frac{1}{2}$. Empty circles, 1; filled squares, 2; filled triangles, 3, 4; filled hexagons, 5, 6; filled inverted triangles, 7, 8; filled circles, 9; empty squares, 10; filled diamonds, 11, 12; empty triangles, 13, 14; empty diamonds, 15, 16. Numeration of faces corresponds to that in Fig. 10. The curves are guides to the eye.

Rotations contribute to the compression of the structure in the *b* direction normal to the pleated layers and also result in an expansion of the structure in particular crystallographic directions in the (*ac*)-plane with increasing pressure, which is most pronounced at pressures above 3.0 GPa. The rotation-induced structural expansion in particular directions was observed despite the fact that the distances between the atoms having short direct contacts in the structure decreased with pressure. This phenomenon is similar to that of bond-angle expansion described previously by Megaw (1939) in relation to thermal expansion of crystals. It may be important to take the observed rotations into consideration when studying the properties of acetaminophen at high pressures. For directional interactions in the crystal, not only the distance changes but also changes in angles (even if they are small) may affect the properties and chemical reactivity to a noticeable extent. In acetaminophen, rotations are interrelated with the perturbations of the hydrogen-bond network and as a consequence may also affect the charge distribution within the acetaminophen molecules (Binev *et al.*, 1998). One can also expect the same or similar rotations and angle distortions to come into play when the crystal structure of acetaminophen is strained as a result of dissolution or sublimation which start locally at the surface, or in the course of polymorph transitions or solid-state chemical reactions.

Owing to cooperative interactions the hydrogen-bonded cycles forming a two-dimensional network in the structure preserve (to a large extent) their size and average shape, despite noticeable relative movements of individual atoms in the cycle. It is important to take into account this cooperativity of the interactions in the hydrogen-bond network (manifesting itself in the high-pressure experiments) when considering processes involving breaking individual hydrogen bonds between the molecules, such as sublimation, dissolution or polymorph transitions.

The monoclinic polymorph of acetaminophen was shown not to be able to undergo any polymorph transition at hydrostatic loading at least up to 4.2 GPa. The hydrogen-bond network and the ability of the molecules to change intramolecular dihedral and torsion angles make it possible to decrease the cell volume retaining the same symmetry group and the packing pattern. However, at 4.0 GPa the molecules were shown to become almost flat, and the OH$\cdots$O and NH$\cdots$O distances, as well as other intermolecular contacts, became very short. Therefore, one can expect that the ability of the structure to decrease its free volume along the same lines is already close to its limit by 5.0 GPa, and a polymorph transition may be expected at a higher pressure.

The study was supported by a grant from the German Federation Ministry of Education, Science and Technology, RUS-131-97, a grant from RFBR (Russia), 99-03-32482, a grant from the Russian Federation Ministry of Education (Russia), 3 H-46-99, and a grant from the Russian Ministry of Science. Dr E. V. Boldyreva gratefully acknowledges financial support from the Alexander von Humboldt Foundation. The authors are grateful to Professor V. V. Boldyrev for stimulating the study and helpful discussions, to N. E. Kashcheeva for the assistance with the usage of the *NADI* program for calculating the Dirichlet domains, and to Dr D. Yu. Naumov for help with using *CAVITY* for preparing plots.

References

Ahsbahs, H. (1984). *Rev. Sci. Instrum.* **55**, 99–102.
Ahsbahs, H. (1987). *Prog. Cryst. Growth Charact.* **14**, 263–302.
Ahsbahs, H., Dorwarth, R., Hölzer, K. & Kuhs, W. F. (1993). *Z. Kristallogr. Suppl.* **7**, 3–4.
Binev, I. G., Vassileva-Boyadjieva, P. & Binev, Yu. I. (1998). *J. Mol. Struct.* **447**, 235–246.
Boldyrev, V. V., Vasilchenko, M. A., Shakhtshneider, T. P., Naumov, D. Y. & Boldyreva, E. V. (1997*a*). *Solid State Ion.* pp. 101–103.
Boldyrev, V. V., Vasilchenko, M. A., Shakhtshneider, T. P., Naumov, D. Y. & Boldyreva, E. V. (1997*b*). *Solid State Ion.* pp. 869–874.
Boldyreva, E. V. (1994). *Mol. Cryst. Liq. Cryst.* **242**, 17–52.
Boldyreva, E. V. (1996). *Reactivity of Solids: Past, Present, Future*, edited by V. V. Boldyrev, pp. 141–184. Oxford: Blackwell Science.
Boldyreva, E. V. (1999). *Reactivity of Molecular Solids*, edited by E. V. Boldyreva & V. V. Boldyrev, pp. 1–50. Chichester: Wiley.
Boldyreva, E. V., Ahsbahs, H., Naumov, D. Y. & Kutoglu, A. (1998). *Acta Cryst.* C**54**, 1378–1383.
Boldyreva, E. V., Ahsbahs, H. & Uchtmann, H. (1994). *Ber. Bunsenges. Phys. Chem.* **98**, 738–745.
Boldyreva, E. V., Kivikoski, J. & Howard, J. A. K. (1997*a*). *Acta Cryst.* B**53**, 394–404.
Boldyreva, E. V., Kivikoski, J. & Howard, J. A. K. (1997*b*). *Acta Cryst.* B**53**, 405–414.
Boldyreva, E. V., Naumov, D. Y. & Ahsbahs, H. (1998*a*). *Acta Cryst.* B**54**, 798–808.
Boldyreva, E. V., Naumov, D. Y. & Ahsbahs, H. (1998*b*). *Zh. Strukt. Khim.* **39**, 433–447 (in Russian).
Clydesdale, G., Docherty, R. & Roberts, K. J. (1991). *Comput. Phys. Commun.* **64**, 311.
Clydesdale, G., Roberts, K. J. & Docherty, R. (1996). *Crystal Growth of Organic Materials*, edited by A. S. Myerson, D. A. Green & P. Meenan, pp. 43–52. Washington, DC: American Chemical Society.
Di Martino, P., Conflant, P., Drache, M., Huvenne, J.-P. & Guyot-Hermann, A. M. (1997). *J. Therm. Analys.* **48**, 447–458.
Finger, L. W. & King, H. (1978). *Am. Mineral.* **63**, 337–342.
Grant, D. & Chow, A. H. (1991). *AIChE Symp. Ser.* **87**, 33–36.
Haisa, M., Kashino, S., Kawai, R. & Maeda, H. (1976). *Acta Cryst.* B**32**, 1283–1285.
Haisa, M., Kashino, S. & Maeda, H. (1974). *Acta Cryst.* B**30**, 2510–2512.
Hazen, R. M. & Finger, L. W. (1982). *Comparative Crystal Chemistry*. New York: Wiley.
Hendriksen, B. A., Grant, D. J. W., Meenan, P. & Green, D. A. (1998). *J. Cryst. Growth*, **183**, 629–640.
Kashcheeva, N. E., Naumov, D. Y. & Boldyreva, E. V. (1999). *Z. Kristallogr.* **214**, 534–541.
Katrusiak, A. (1990). *Acta Cryst.* B**46**, 246–256.
Katrusiak, A. (1991*a*). *Cryst. Res. Techn.* **26**, 523–531.
Katrusiak, A. (1991*b*). *High Press. Res.* **6**, 155–167.
Katrusiak, A. (1991*c*). *High Press. Res.* **6**, 265–275.
Katrusiak, A. (1995). *Acta Cryst.* B**51**, 873–879.
Katrusiak, A. (1996). *Cryst. Rev.* **5**, 133–180.
Katrusiak, A. & Nelmes, R. J. (1986). *J. Phys. C*, **19**, L765–772.
Kutoglu, A. (1997). *MDIF4.* Marburg University, Germany.
Mao, K. H. & Bell, P. M. (1980). *Carnegie Inst. Yearb. 79*, pp. 409–411.
Megaw, H. D. (1939). *Z. Kristallogr.* **100**, 58–76.
Merck Index (1976). *Merck Index*, 9th ed., p. 6. Rahway, NY: Merck & Co.

Merrill, L. & Bassett, W. A. (1974). *Rev. Sci. Instrum.* **45**, 290–294.
Naumov, D. Yu. & Boldyreva, E. V. (1997). *Proceedings of the Russian National Conference of the Application of X-rays, Synchrotron Radiation, Neutrons and Electrons for Studies of Materials*, p. 608. Dubna: United Institute of Nuclear Research.
Naumov, D. Yu. & Boldyreva, E. V. (1999). *Zh. Strukt. Khim.* **40**, 102–110 (in Russian).
Naumov, D. Y., Vasilchenko, M. A. & Howard, J. A. K. (1998). *Acta Cryst.* C**54**, 653–655.
Nichols, G. & Frampton, C. S. (1998). *J. Pharm. Sci.* **87**, 684–693.
Piermarini, G. J., Block, S., Barnett, J. D. & Forman, R. A. (1975). *J. Appl. Phys.* **46**, 2774–2780.
Shakhtshneider, T. P., Boldyreva, E. V., Vasilchenko, M. A., Ahsbahs, H. & Uchtmann, H. (1998). *Dokl. Ross. Akad. Nauk.* **363**, 783–786.
Shakhtshneider, T. P., Boldyreva, E. V., Vasilchenko, M. A., Ahsbahs, H. & Uchtmann, H. (1999). *Zh. Strukt. Khim.* **40**, 1140–1148 (in Russian).
Sheldrick, G. (1997). *SHELX*97. University of Göttingen, Germany.
Shekunov, B. Yu., Aulton, M. E., Adama-Acquah, R. W. & Grant, D. J. W. (1996). *J. Chem. Soc. Faraday Trans.* **92**, 439–444.
Sowa, H. (1994). *Z. Kristallogr.* **209**, 954–960.
Vasilchenko, M. A., Shakhtshneider, T. P., Naumov, D. Y. & Boldyrev, V. V. (1996). *Dokl. Ross. Akad. Nauk.* **350**, 777–780.
Vasilchenko, M. A., Shakhtshneider, T. P., Naumov, D. Y. & Boldyrev, V. V. (1997). *J. Pharm. Sci.* **85**, 929–934.